Calculation of the pion's quark distribution amplitude in lattice QCD with dynamical fermions

D. Daniel

T-8 (MS-B285), Los Alamos National Laboratory, Los Alamos, New Mexico 87545*
and Physics Department, University of Edinburgh, Edinburgh EH9 3JZ, Scotland

R. Gupta

T-8 (MS-B285), Los Alamos National Laboratory, Los Alamos, New Mexico 87545

D. G. Richards

Physics Department, University of Edinburgh, Edinburgh EH9 3JZ, Scotland
(Received 3 December 1990)

We present a calculation of the pion decay constant and of the second moment of the quark distribution amplitude of the pion within full lattice QCD. Measurements are made on $12^3 \times 24$ and $16^3 \times 32$ lattices, using two flavors of Wilson fermion. Different methods used to extract f_π give consistent results. We find a better signal for the second moment of the distribution amplitude than in previous lattice calculations and obtain results that are significantly smaller than those obtained from sum-rule calculations and previously in (quenched) lattice QCD.

I. INTRODUCTION

In the approach of Lepage and Brodsky[1] to exclusive hadronic processes at large momentum transfer (high Q^2), the scattering amplitude is approximated by the convolution of a perturbatively calculable hard-scattering amplitude with wave functions describing the overlap of the participating hadrons with their lowest Fock state. These wave functions—the quark distribution amplitudes in the hadron—are hypothesized to contain the relevant nonperturbative physics. This factorization remains controversial, as we shall discuss below.

In this paper we specialize to the case of the pseudoscalar mesons. The momentum-space quark and antiquark distribution amplitude ϕ depends on $\xi \equiv x_q - x_{\bar{q}}$, where x_q and $x_{\bar{q}}$ are the fractional light-cone momenta carried by the quark and antiquark, respectively, as well as on the renormalization scale Q^2 at which the wave function is defined. The general features of $\phi(\xi, Q^2)$ can be deduced from its moments

$$\langle \xi^n \rangle = \int_{-1}^{1} d\xi \, \xi^n \phi(\xi, Q^2) \ . \tag{1.1}$$

ϕ is normalized such that $\langle \xi^0 \rangle = 1$. Note that odd moments vanish by parity. The moments are related to the matrix elements of the local operators

$$O^{(n)}_{\mu_0 \mu_1 \cdots \mu_n} = (-i)^n \bar{\psi} \gamma_5 \gamma_{\mu_0} \vec{D}_{\mu_1} \vec{D}_{\mu_2} \cdots \vec{D}_{\mu_n} \psi \ , \tag{1.2}$$

through the operator-product expansion, giving

$$\langle 0 | O^{(n)}_{\mu_0 \mu_1 \cdots \mu_n} | \pi(p) \rangle = f_\pi p_{\mu_0} p_{\mu_1} \cdots p_{\mu_n} \langle \xi^n \rangle \ , \tag{1.3}$$

where $f_\pi = 132$ MeV is the pion decay constant. The operators are understood to be traceless. To study their renormalization it is convenient to symmetrize over Lorentz indices, but Eq. (1.3) holds in any case, as a

consequence of Lorentz covariance. The Q^2 dependence of these matrix elements is calculable within perturbation theory, and consequently the large-Q^2 form of the wave function is known. At accessible energy scales nonperturbative techniques are necessary to determine $\phi(\xi, Q^2)$.

One way of extracting information about the form of the wave function without resorting to lattice-gauge-theory simulations is to estimate the moments using sum-rule methods. The study of the first few moments by Chernyak and Zhitnitsky[2] yielded values for the moments consistent with the "camel-shaped" form of the wave function,

$$\phi[\xi, Q^2 = (0.5 \text{ GeV})^2] = \tfrac{15}{4} \xi^2 (1 - \xi^2) \ , \tag{1.4}$$

in which there is a large amplitude for most of the pion's momentum to be carried by either the quark or the antiquark, with the remaining parton carrying little momentum. In particular they found $\langle \xi^2 \rangle \approx 0.4$ at $Q^2 = 1.5$ GeV^2.

The estimate in Ref. 2 is based on the conventional application of sum rules: The nonperturbative information is assumed to be encoded in a small number of vacuum expectation values of *local operators* (local condensates). If, on the other hand, the sum-rule method is generalized to include *nonlocal* condensates, the estimate for $\langle \xi^2 \rangle$ is reduced, and is very sensitive to the precise form of the nonlocal condensate. Using this generalized method Mikhailov and Radyushkin[3] conclude that $\langle \xi^n \rangle < 1/(1+n)$, suggesting that ϕ does not have a minimum at $\xi = 0$. There are objections to the whole Lepage-Brodsky program, however. Isgur and Llewellyn-Smith[4] argue that perturbation theory remains inapplicable for exclusive processes, except perhaps for extremely high energies. In diagrammatic language this is because large pion momentum does not guarantee large momentum flow in all internal lines. This situation is exacerbated if the pion's quark

distribution amplitude really is camel shaped.

The calculation of ϕ nonperturbatively from first principles therefore remains an important and outstanding problem. Lattice QCD provides a method to approach this (though at present only $\langle \xi^2 \rangle$ is tractable). In previous calculations using the quenched approximation, this has proved a difficult quantity to measure. The results obtained were

$$\langle \xi^2 \rangle_{\text{latt}} = 0.26 \pm 0.13 \quad \text{(Martinelli and Sachrajda[5])}$$
$$\langle \xi^2 \rangle_{\text{latt}} = 0.30 \pm 0.13 \quad \text{(DeGrand and Loft[6])} ,$$
(1.5)

where the subscript indicates that these numbers do not include the renormalization constant which relates lattice and continuum measurements. This constant is not known precisely, but will increase the lattice results by a factor of around 1.2–1.4. Given the large errors, the above results cannot distinguish between the sum-rule estimate of Ref. 2, or the bound of Ref. 3; nor can it rule out $\langle \xi^2 \rangle = 0.2$, which is characteristic of the $Q^2 \to \infty$ limit, $\phi(\xi, Q^2 = \infty) = \frac{3}{4}(1 - \xi^2)$.

This paper contains the results of a calculation of the pion decay constant and the second moment of the quark distribution amplitude of the pion. In the case of $\langle \xi^2 \rangle$, the three improvements over previous lattice calculations are (a) we use a "smeared" source for the pion in an attempt to improve the signal, (b) we use a larger spatial volume, and (c) we include the effect of two flavors of (admittedly rather massive) sea quark.

In what follows we review the method for extracting the relevant matrix elements from lattice QCD, discuss the configurations that we have analyzed, and describe our measurements and error analysis. We then present our results and discuss their implications. Briefly, we find that estimates of f_π obtained using different matrix elements are consistent with one another, and in good agreement with physical expectations. However, we find that $\langle \xi^2 \rangle$ is smaller than previous (quenched) lattice QCD calculations, and the sum-rule calculation of Ref. 2.

II. MATRIX ELEMENTS FROM LATTICE CALCULATIONS

In this section we review the method for extracting the relevant matrix elements, Eq. (1.3), from lattice QCD.[5] We examine the large-time behavior of the correlators

$$K_{\mu_0\mu_1\cdots\mu_n}(t,\mathbf{p})$$
$$= \sum_{\mathbf{x}} e^{i\mathbf{p}\cdot\mathbf{x}} \langle O^{(n)}_{\mu_0\mu_1\cdots\mu_n}(\mathbf{x},t) J(0,0)^\dagger \rangle , \quad (2.1)$$

$$C(t,\mathbf{p}) = \sum_{\mathbf{x}} e^{i\mathbf{p}\cdot\mathbf{x}} \langle J(\mathbf{x},t) J(0,0)^\dagger \rangle , \quad (2.2)$$

where $J(x) \equiv \pi(x) = \bar{\psi}(x)\gamma_5\psi(x)$ or $J(x) \equiv A_4(x) = \bar{\psi}(x)\gamma_5\gamma_4\psi(x)$ are two local interpolating operators for the pion, and $O^{(n)}_{\mu_0\mu_1\cdots\mu_n}(x)$ is a lattice transcription of the continuum operator, Eq. (1.2), centered about the lattice point x. Far from the source, these correlators are dominated by the propagation of the lightest particle having an overlap with the interpolating operators; so that

$$K_{\mu_0\mu_1\cdots\mu_n}(t,\mathbf{p}) \sim e^{-E(\mathbf{p})t} \frac{1}{2E(\mathbf{p})} \langle 0|O^{(n)}_{\mu_0\mu_1\cdots\mu_n}(0)|\pi(p)\rangle$$
$$\times \langle \pi(p)|J(0)^\dagger|0\rangle , \quad (2.3)$$

$$C(t,\mathbf{p}) \sim e^{-E(\mathbf{p})t} \frac{1}{2E(\mathbf{p})} |\langle 0|J(0)|\pi(p)\rangle|^2 , \quad (2.4)$$

where $E(\mathbf{p}) \approx (\mathbf{p}^2 + m_\pi^2)^{1/2}$. For periodic boundary conditions there is a similar contribution from the propagation of the particle backwards around the lattice.

To measure f_π we need the lattice operator $O^{(0)}_\mu(x)$, which is nothing but the local axial-vector current A_μ. For $\langle \xi^2 \rangle$, we also require $O^{(2)}_{\mu_0\mu_1\mu_2}(x)$, whose definition on the lattice requires care.

On the lattice the Euclidean symmetry of the continuum is replaced by the hypercubic group. This leads to the problem that operators of different dimensions transform as the same irreducible representation. Consequently, there can be mixing between operators, leading to power divergences that are lattice artifacts. In particular, the simple zero-momentum operator $O^{(2)}_{\mu\mu\mu}(x)$ mixes with $O^{(0)}_\mu(x)$ with a quadratically divergent coefficient. There are two ways of tackling this problem. First the mixing coefficients can be calculated explicitly using lattice perturbation theory. This "perturbative subtraction" method was used in the first distribution amplitude measurements.[7] Alternatively, the Lorentz indices on the operator can be chosen so as to circumvent this mixing.[5] The discrepancies between the results obtained using the two techniques, and the question of the applicability of perturbation theory to these problems, have been comprehensively discussed in Refs. 5 and 6. Their conclusion is that perturbative subtraction does not work for $g^2 \approx 1$. We therefore adopt the second method.

In this method there are two different choices of operators, both of which require that the pion be at nonzero spatial momentum. In the first case we set, say, p_3 to be nonzero, and compute

$$K_{433}(t,\mathbf{p}) - \frac{1}{2}[K^{(2)}_{422}(t,\mathbf{p}) + K^{(2)}_{411}(t,\mathbf{p})]$$
$$\Longrightarrow f_\pi p_4 p_3 p_3 \langle \xi^2 \rangle . \quad (2.5)$$

In the second case we set two components of momenta, say p_2 and p_3, to be nonzero and compute

$$K_{423}(t,\mathbf{p}) \Longrightarrow f_\pi p_4 p_2 p_3 \langle \xi^2 \rangle . \quad (2.6)$$

We make use of the spatial symmetry of the lattice to improve the statistics by averaging over the possible spatial indices (with momentum chosen accordingly).

The results extracted in this way are still not precisely what we want, because they are the matrix elements of operators defined in the lattice regularization scheme. To obtain numbers of physical interest we must relate them to operators in a continuum scheme. In the absence of mixing, the continuum operators are given by $O = ZO^{\text{latt}}$, where Z includes terms which cancel any logarithmic divergence in a of the lattice operator. In our case we need the renormalization constants of three operators: A_μ, $O^{(2)}_{433}$, and $O^{(2)}_{423}$. In perturbation theory, assuming tadpoles are the dominant contribution, these (at $g^2 \approx 1$) are $Z_A \approx 0.85$ for the axial-vector current, and $Z_O \approx 1.15$

for the other two operators (though there will be a slight difference between them). Unfortunately, quenched simulations have shown that perturbation theory is not a reliable guide for $g^2 \approx 1$.[8] A more reasonable estimate for Z_A is 0.8, a value which we will adopt below. For Z_O something in the range 1.1–1.3 is a reasonable guess. In terms of Z_A and Z_O, the numbers we actually extract are

$$f_\pi^{\text{latt}} = \frac{1}{Z_A} f_\pi ,$$

$$\langle \xi^2 \rangle^{\text{latt}} = \frac{Z_A}{Z_O} \langle \xi^2 \rangle . \qquad (2.7)$$

For the time being, the uncertainty in the values of Z_A and Z_O remains a weakness in the calculation.

In this study we have used operators $O^{(n)}$ symmetrized over all indices as in Refs. 5 and 6. However, we do not believe this is necessary in order to avoid the problem of mixing with lower-dimension operators. In particular $O_{433} - O_{422}$ with or without symmetrization belongs to the 8 irreducible representation of the hypercubic group and so cannot mix with O_4. We believe that the unsymmetrized operator will have a better signal since it lives on a single time slice. We are in the process of testing this hypothesis. With the operator O_{423} also, one need symmetrize only over the spatial indices.

III. DETAILS OF THE SIMULATIONS

This analysis is based on a simulation of the full QCD theory using two degenerate flavors of Wilson fermion. Configurations of size 12^4 and 16^4 were generated using the hybrid Monte Carlo algorithm,[9] and quark propagators were subsequently calculated on these lattices after replicating once in the time direction. Full details of the simulations are contained in Ref. 10, but the parameters for the configurations used in these measurements are shown in Table I. Lattices are analyzed approximately every 20 time units with an average acceptance rate of about 70%. We find that the lightest value of the pion mass attained in these simulations is approximately 600 MeV, and therefore we expect the effect of including dynamical quarks in these simulations to be small compared to the physical world.

It should be pointed out that the update in the hybrid Monte Carlo runs on the 16^4 lattices has the following error: The random number generator used in the crucial Metropolis accept-reject step was by default initialized with the same starting seed at the beginning of each restart of the job. (Note that a separate parallel random-number generator is used for the hybrid update; so the trajectories themselves are correct.) Since a large fraction of the time of each run consisted of a few trajectories, using the same sequence is expected to produce a bias. Consequently, the resulting update was closer in spirit to simple hybrid update, which is what would be obtained in the limit of 100% acceptance. Since fixing this bug, we have generated 150 trajectories at each of the two lightest quark mass values, $\beta = 5.5$, $\kappa = 0.160$ and $\beta = 5.6$, $\kappa = 0.157$, and we do not notice any systematic shift in the results. So, we believe that the bias generated by using the same random-number sequence is of the same order as the statistical errors. Also, we find similar results for the 12^4 lattices (which were run on a Cray and do not have a bias). The more severe limitation of this calculation is that we have very few decorrelated lattices in our statistical sample.[10]

The quark propagators were computed from a "smeared" source at a fixed time slice t_0. The smearing method adopted was that of Ref. 11, in which the source $S(\mathbf{x})$ is the solution of the scalar three-dimensional gauge-covariant Klein-Gordon equation:

$$(-\mathbf{D}^2 + m_s^2) S(\mathbf{x}) = \delta_{\mathbf{x}0} . \qquad (3.1)$$

The tunable parameter m_s may be regarded as a "constituent" quark mass. This gauge-invariant procedure gives (for appropriately chosen m_s) a large overlap with the wave functions of low-lying hadronic states so that they dominate the behavior of correlation functions after only a few time slices. In this calculation m_s was chosen to give a smearing radius of approximately 4 lattice units, and in Table I we give the value of time separation at which the pion dominates the correlation function. We plan to experiment with different smearing techniques in

TABLE I. The parameters used in the simulations. Lattices are of size L^4, doubled to $L^4 \times 2L$, N is the number of configurations in the sample, t_π is the time slice at which the pion saturates correlators, m_π is given in lattice units, and a^{-1} is the approximate inverse lattice spacing by extrapolation of m_ρ to the chiral limit. The final column gives the value of the pion decay constant in lattice units as calculated in this paper.

β	L	κ	N	t_π	m_π	$(m_\pi/m_\rho)^2$	a^{-1} GeV	$Z_A^{-1} f_\pi$
5.4	12	0.160	15	3	0.767(14)	0.78(4)	1.5	0.212(12)
5.4	12	0.161	15	4	0.658(13)	0.75(6)	1.5	0.178(21)
5.4	16	0.162	14	7	0.580(7)	0.64(4)	1.5	0.162(8)
5.5	16	0.158	15	6	0.569(5)	0.72(2)	1.8	0.152(7)
5.5	16	0.159	17	7	0.479(4)	0.64(2)	1.8	0.129(6)
5.5	16	0.160	26	8	0.355(10)	0.48(3)	1.8	0.114(5)
5.6	16	0.156	21	7	0.462(7)	0.66(3)	2.4	0.126(5)
5.6	16	0.157	32	9	0.360(7)	0.61(3)	2.4	0.102(4)

the future.

For the determination of the matrix element of the distribution amplitude operators through Eq. (2.1), the quark propagators from a smeared source to a point sink were employed. This is because the relationship between the matrix element of the operators $O^{(n)}_{\mu_0\mu_1\cdots\mu_n}(x)$ calculated with a quark propagator smeared at the point x and the corresponding matrix element calculated using an unsmeared propagator is unknown. We call these propagators "smeared local" and label the corresponding correlators with SL. To calculate f_π we also need to determine the matrix element $\langle 0|J|\pi(\mathbf{p})\rangle$ from Eq. (2.4). This requires the calculation of propagators smeared at both the source and sink x. We call such propagators "smeared smeared" and label the corresponding correlators by SS.

For the estimate of f_π we used two methods. In method 1 we fit to the ratio of K^{SL}_μ and the pion correlator C^{SS} to cancel the exponential falloff. The amplitude at the source, which we need to remove, is obtained from an independent fit to C^{SS}. In method 2, we determine the amplitude and energy from separate single-particle fits to the correlators K^{SL}_μ and C^{SS}. In this way we extract five parameters: A_{SL}, E_{SL}, A_{SS}, E_{SS}, and R, where we assume that the long-time behavior of the correlator is of the form $A\exp(-Et)$ and R is the ratio extracted directly. The final value of f_π is given by

$$\frac{1}{Z_A}f^1_\pi=R\frac{E_{SL}}{p_\mu}\left[\frac{2A_{SS}}{E_{SS}}\right]^{1/2},$$

$$\frac{1}{Z_A}f^2_\pi=\frac{2A_{SL}E_{SL}}{p_\mu\sqrt{2A_{SS}E_{SS}}}$$

(3.2)

for the two methods. We have carried out this analysis with and without pion momenta and with both spatial and time components of the axial-vector current. We find that method 1 gives more stable results, and the best estimate is obtained using the time component of the axial-vector current and at zero momentum, as discussed in the next section.

To estimate $\langle\xi^2\rangle$ we fit to the ratio of the second-order correlators defined in Eqs. (2.5) and (2.6), and the lowest-order correlator:

$$R^{433}_4\equiv\frac{K^{SL}_{433}-\frac{1}{2}(K^{SL}_{411}+K^{SL}_{422})}{K^{SL}_4}\sim p_3p_3\langle\xi^2\rangle_{\text{latt}},$$

$$R^{423}_4\equiv\frac{K^{SL}_{423}}{K^{SL}_4}\sim p_2p_3\langle\xi^2\rangle_{\text{latt}},$$

$$R^{433}_3\equiv\frac{K^{SL}_{433}-\frac{1}{2}(K^{SL}_{411}+K^{SL}_{422})}{K^{SL}_3}\sim p_4p_3\langle\xi^3\rangle_{\text{latt}},$$

(3.3)

$$R^{423}_3\equiv\frac{K^{SL}_{423}}{K^{SL}_3}\sim p_4p_2\langle\xi^2\rangle_{\text{latt}},$$

where $\langle\xi^2\rangle_{\text{latt}}=Z_AZ_O^{-1}\langle\xi^2\rangle$. For the last two ratios we also fit to K^{SL}_3 to determine the energy p_4. We find comparable signals in all four channels, though the quality has considerable variation presumably due to limited statistics. We can also estimate $\langle\xi^2\rangle$ by making separate fits to the numerator and denominator (analogous to method 2 for f_π). However, we find a poor signal in the numerator, so the signal we obtain in the ratio depends crucially on a cancellation of fluctuations. As a test of our calculation we verify that the first moment of the quark distribution amplitude in the pion vanishes.

The method used to make the fits is as follows: We first examine the effective mass plot to determine the range of fit over which the pion saturates the two-point correlator. We then use a single elimination "jackknife" method[12] calculating χ^2 for each sample using the correlated covariance matrix. In method 2 described above, we also tuned the range of t to which the data were fit so that the ratio of energies is consistent with unity.

We briefly review the construction of the covariance matrix and χ^2 function for ratios of correlators, as it may not be familiar to all of our readers. A single correlator $C(t)$ is a set of averages over configurations of some quantities $x_n(t)$:

$$C(t)=\langle x(t)\rangle\equiv\sum_{n=1}^N x_n(t)/N,$$

where N is the number of configurations. Correlations between time slices are characterized by the covariance matrix

$$\mathbf{V}(t,t')=\frac{1}{N^2}\sum_{n=1}^N[x_n(t)-\langle x(t)\rangle][x_n(t')-\langle x(t')\rangle].$$

(3.4)

A fit of $C(t)$ to a functional form $f(t;\{\alpha\})$ over the range $[t_{\min},t_{\max}]$ taking correlations into account can then be made by minimizing

$$\chi^2=\sum_{t,t'=t_{\min}}^{t_{\max}}[C(t)-f(t;\{\alpha\})]\mathbf{V}^{-1}(t,t')$$

$$\times[C(t')-f(t';\{\alpha\})],$$

(3.5)

with respect to the parameters $\{\alpha\}$. The smaller the minimal value of χ^2, the better the fit. For a ratio of correlators, $R(t)=\langle x(t)\rangle/\langle y(t)\rangle$, we treat $x_n(t)-\langle x(t)\rangle$ as a differential and derive the covariance matrix

$$\mathbf{V}(t,t')=\frac{1}{N^2}\sum_{n=1}^N R(t)R(t')\left[\frac{x_n(t)-\langle x(t)\rangle}{\langle x(t)\rangle}-\frac{y_n(t)-\langle y(t)\rangle}{\langle y(t)\rangle}\right]\left[\frac{x_n(t')-\langle x(t')\rangle}{\langle x(t')\rangle}-\frac{y_n(t')-\langle y(t')\rangle}{\langle y(t')\rangle}\right]$$

$$=\frac{1}{N^2}\sum_{n=1}^N R(t)R(t')\left[\frac{x_n(t)}{\langle x(t)\rangle}-\frac{y_n(t)}{\langle y(t)\rangle}\right]\left[\frac{x_n(t')}{\langle x(t')\rangle}-\frac{y_n(t')}{\langle y(t')\rangle}\right].$$

(3.6)

To perform a correlated fit we again minimize the χ^2 function, which is defined as before but with $C(t)$ replaced by $R(t)$. Covariance matrices and χ^2 functions for fitting arbitrary functions of correlators may be constructed in a similar manner.

Finally we mention that a more satisfactory way of extracting f_π would be to perform a simultaneous correlated fit to C^{SS} and K_μ^{SL} with three free parameters A_{SL}, A_{SS}, and E:

$$C^{SS}(t) \sim A_{SS}\exp(-Et), \quad K_\mu^{SL} \sim A_{SL}\exp(-Et). \quad (3.7)$$

For a given time interval t_{fit}, this requires fitting to $2t_{fit}$ data points with the constraint that for an invertible covariance matrix $2t_{fit} \leq N$ where N is the number of configurations. In practice we find that the covariance matrix develops small eigenvalues much before this singular limit, and in our experience the resulting fit is not reliable. Since at most β and κ values we have only 15 or so configurations, the quality of our data would re-

strict us to $t_{fit} < 6$. For this reason we choose to postpone the use of simultaneous correlated fits until a larger ensemble of configurations is available.

IV. RESULTS

We begin the discussion of the results with the extraction of the lattice pion decay constant f_π using $C^{SS}(t,\mathbf{p})$ and $K_\mu^{SL}(t,\mathbf{p})$. We show the results at $\beta=5.4$, 5.5, and 5.6 in Tables II–IV, respectively. At each value of β and κ we have up to six independent estimates depending on the choice of operators O_μ and J and the momentum, as indicated in the first column. We also use the two different methods described in Sec. III. Each of these requires extracting the energies, amplitudes, and ratio of amplitudes from fits to pion correlators, and these are given in Columns 2–6. For the lightest pion mass at each β value we also quote the fit range used and χ^2 per degree of freedom achieved for the determination of these parameters. A consistency check is that the energies of the

TABLE II. The measured values of the parameters required for the determination of f_π [see Eq. (3.2)], together with the two resulting estimates for $Z_A^{-1}f_\pi$ (in lattice units) are shown at various values of spatial momentum (indicated in integer units) for $\beta=5.4$. At $\kappa=0.162$ we quote the fit range used and χ^2 per degree of freedom in addition to the fit parameter(s).

$O_\mu J(\mathbf{p})$	$A_{SS}\times 10^{-4}$	E_{SS}	$A_{SL}\times 10^{-1}$	E_{SL}	$R\times 10^2$	E_{SL}/E_{SS}	f_π^1	f_π^2
			f_π from $n_f=2$ Wilson fermions at $\beta=5.4$					
			$\kappa_d=0.160$; 15 $12^4 \rightarrow 12^3\times 24$ lattices					
$A_4\pi(000)$	3.495(240)	0.767(14)	2.675(220)	0.781(12)	0.070(3)	1.02	0.212(12)	0.231(21)
$A_4\pi(100)$	1.339(140)	0.919(23)	1.797(180)	0.922(18)	0.128(7)	1.00	0.218(16)	0.229(26)
$A_4\pi(110)$	0.581(94)	0.997(47)	1.096(140)	1.017(21)	0.200(23)	1.02	0.216(31)	0.204(31)
$A_i\pi(100)$	1.339(140)	0.919(23)	0.969(71)	0.910(21)	0.068(2)	0.99	0.203(13)	0.215(20)
$A_i\pi(110)$	0.581(94)	0.997(47)	0.447(89)	0.991(50)	0.094(3)	0.99	0.191(20)	0.157(35)
			$\kappa_d=0.161$; 15 $12^4 \rightarrow 12^3\times 24$ lattices					
$A_4\pi(000)$	4.753(820)	0.658(13)	2.528(270)	0.657(13)	0.047(4)	1.00	0.178(21)	0.202(28)
$A_4\pi(100)$	1.588(130)	0.811(16)	1.605(150)	0.816(25)	0.077(4)	1.01	0.151(10)	0.200(20)
$A_4\pi(110)$	0.587(45)	0.915(37)	1.121(170)	0.952(39)	0.130(15)	1.04	0.147(18)	0.216(34)
$A_i\pi(100)$	1.588(130)	0.811(16)	0.843(57)	0.805(21)	0.050(3)	0.99	0.152(12)	0.161(14)
$A_i\pi(110)$	0.587(45)	0.915(37)	0.476(40)	0.919(27)	0.068(5)	1.00	0.134(11)	0.161(16)
			$\kappa_d=0.162$; 14 $16^4 \rightarrow 16^3\times 32$ lattices					
	9–15		6–12		6–12			
	2.37		1.14		2.24			
$A_4 A_4(000)$	0.158(38)	0.582(29)	0.375(52)	0.582(13)	0.214(4)	1.00	0.158(20)	0.175(32)
	6–13		6–13		8–12			
	1.16		2.36		2.30			
$A_4\pi(000)$	0.772(57)	0.582(4)	0.694(89)	0.578(15)	0.101(1)	0.99	0.164(6)	0.146(20)
	6–13		4–10		4–11			
	2.00		1.13		2.92			
$A_4\pi(100)$	0.389(41)	0.679(11)	0.619(79)	0.686(16)	0.148(3)	1.01	0.158(9)	0.170(24)
	6–13		5–13		5–12			
	2.69		1.36		4.53			
$A_4\pi(110)$	0.310(42)	0.795(19)	0.652(110)	0.801(19)	0.196(6)	1.01	0.173(13)	0.186(34)
	6–13		8–14		6–11			
	2.00		3.54		1.00			
$A_i(100)$	0.389(41)	0.679(11)	0.314(21)	0.673(12)	0.077(2)	0.99	0.141(9)	0.148(13)
	6–13		7–14		5–11			
	2.69		1.44		0.57			
$A_i\pi(110)$	0.310(42)	0.795(19)	0.234(26)	0.776(18)	0.092(4)	0.98	0.160(13)	0.132(17)

SS and SL correlators agree. We show the ratio of these energies in Column 7. In most cases they agree to within a few percent. In Fig. 1 we show as an example the ratio plot for $\beta=5.5$ and $\kappa=0.160$ corresponding to the lightest pion mass.

The best estimate is derived from the zero-momentum correlators, and the weighted mean of these estimates using f_π^1 is given in the last column of Table I. We regard the second estimate f_π^2 to be a consistency check. Also, note that on the 12^4 lattices we do not have the estimate from the A_4A_4 correlators. The measurements presented in this paper were obtained on sets of configurations at various values of β and κ, and thus at a variety of lattice spacings. To present the data in an intelligible form, and to eliminate the uncertainty in the lattice spacing, we show in Fig. 2 the data for $Z_A^{-1}f_\pi/m_\rho$ against $(m_\pi/m_\rho)^2$. In this graph we also plot the physical points

for the pion and kaon [where the appropriate vector meson is $K^*(892)$], and these points rescaled by the lattice axial-vector-current renormalization constant which, as discussed in Sec. II, we take to be $Z_A=0.8$. Our results show that $Z_A^{-1}f_\pi/m_\rho$ is within errors independent of β and the quark mass (which is evidence for scaling) and in agreement with the rescaled physical value.

As shown in Tables II–IV f_π is within errors independent of the momentum. This is evidence that for small momenta Euclidean symmetry is respected to a good approximation. To give an idea of the coarseness of the lattice, the two smallest nonzero momenta have modulus $p=2\pi/aL$ and $p=2\sqrt{2}\pi/aL$. For $L=12$ these correspond to $ap=0.524$ and $ap=0.740$, whereas for $L=16$ we have $ap=0.393$ and $ap=0.555$.

As ap approaches unity, we expect the granularity of the lattice to be increasingly apparent, and the correla-

TABLE III. The measured values of the parameters required for the determination of f_π [see Eq. (3.2)], together with the two resulting estimates for $Z_A^{-1}f_\pi$ (in lattice units) are shown at various values of spatial momentum (indicated in integer units) for $\beta=5.5$. At $\kappa=0.160$ we quote the fit range used and χ^2 per degree of freedom in addition to the fit parameter(s).

$O_\mu J(\mathbf{p})$	$A_{SS}\times10^{-4}$	E_{SS}	$A_{SL}\times10^{-1}$	E_{SL}	$R\times10^2$	E_{SL}/E_{SS}	f_π^1	f_π^2
			f_π from $n_f=2$ Wilson fermions at $\beta=5.5$					
			$\kappa_d=0.158$; 15 $16^4\to16^3\times32$ lattices					
$A_4A_4(000)$	0.325(28)	0.569(8)	0.398(45)	0.565(9)	0.141(2)	0.99	0.150(7)	0.131(16)
$A_4\pi(000)$	1.170(80)	0.567(4)	0.859(88)	0.566(7)	0.075(1)	1.00	0.153(6)	0.149(16)
$A_4\pi(100)$	0.624(51)	0.687(10)	0.746(80)	0.691(11)	0.116(2)	1.01	0.156(7)	0.161(19)
$A_4\pi(110)$	0.471(97)	0.815(31)	0.688(80)	0.815(13)	0.157(2)	1.00	0.169(18)	0.157(25)
$A_i\pi(100)$	0.624(51)	0.687(10)	0.356(27)	0.671(7)	0.059(1)	0.98	0.136(6)	0.131(11)
$A_i\pi(110)$	0.471(97)	0.815(31)	0.280(37)	0.795(24)	0.070(2)	0.98	0.153(17)	0.129(22)
			$\kappa_d=0.159$; 17 $16^4\to16^3\times32$ lattices					
$A_4A_4(000)$	0.270(29)	0.478(6)	0.318(55)	0.472(12)	0.122(1)	0.99	0.129(7)	0.125(23)
$A_4\pi(000)$	1.272(83)	0.479(4)	0.700(81)	0.480(10)	0.056(1)	1.00	0.129(5)	0.127(15)
$A_4\pi(100)$	0.716(79)	0.657(15)	0.810(75)	0.667(11)	0.106(3)	1.01	0.157(10)	0.167(18)
$A_4\pi(110)$	0.419(64)	0.769(26)	0.657(80)	0.782(18)	0.150(8)	1.02	0.157(15)	0.164(24)
$A_i\pi(100)$	0.716(79)	0.657(15)	0.288(30)	0.661(13)	0.056(2)	1.01	0.139(10)	0.100(12)
$A_i\pi(110)$	0.419(64)	0.769(26)	0.649(75)	0.781(16)	0.070(3)	1.02	0.146(14)	0.321(45)
			$\kappa_d=0.160$; 26 $16^4\to16^3\times32$ lattices					
	7–15		7–15		7–16			
	1.35		1.66		2.48			
$A_4A_4(000)$	0.247(21)	0.373(7)	0.238(17)	0.363(9)	0.101(1)	0.97	0.116(5)	0.111(9)
	7–15		6–13		6–13			
	0.59		1.98		1.08			
$A_4\pi(000)$	1.495(10)	0.355(10)	0.631(26)	0.365(7)	0.039(1)	1.03	0.112(5)	0.122(7)
	6–13		7–15		7–11			
	2.86		1.07		0.40			
$A_4\pi(100)$	0.660(93)	0.556(24)	0.609(99)	0.557(20)	0.077(3)	1.00	0.119(10)	0.142(25)
	7–15		5–11		6–12			
	0.76		1.17		0.65			
$A_4\pi(110)$	0.360(120)	0.663(42)	0.452(76)	0.666(25)	0.119(6)	1.00	0.124(22)	0.131(31)
	6–13		5–11		6–12			
	2.86		0.80		3.00			
$A_i\pi(100)$	0.660(93)	0.556(24)	0.357(35)	0.536(17)	0.054(3)	0.96	0.114(12)	0.114(14)
	7–15		5–11		6–14			
	0.76		2.39		1.55			
$A_i\pi(110)$	0.360(120)	0.663(42)	0.186(23)	0.611(22)	0.071(4)	0.92	0.114(21)	0.084(18)

TABLE IV. The measured values of the parameters required for the determination of f_π [see Eq. (3.2)], together with the two resulting estimates for $Z_A^{-1}f_\pi$ (in lattice units) are shown at various values of spatial momentum (indicated in integer units) for $\beta = 5.6$. At $\kappa = 0.157$ we quote the fit range used and χ^2 per degree of freedom in addition to the fit parameter(s).

$O_\mu J(\mathbf{p})$	$A_{SS} \times 10^{-4}$	E_{SS}	$A_{SL} \times 10^{-1}$	E_{SL}	$R \times 10^2$	E_{SL}/E_{SS}	f_π^1	f_π^2
			f_π from $n_f = 2$ Wilson fermions at $\beta = 5.6$					
			$\kappa_d = 0.156$; 12 $16^4 \to 16^3 \times 32$ lattices					
$A_4 A_4(000)$	0.083(7)	0.466(7)	0.189(19)	0.461(8)	0.209(2)	0.99	0.125(6)	0.136(15)
$A_4\pi(000)$	0.381(22)	0.464(6)	0.363(25)	0.457(7)	0.099(1)	0.98	0.127(4)	0.122(9)
$A_4\pi(100)$	0.244(23)	0.635(15)	0.336(29)	0.627(12)	0.155(4)	0.99	0.136(8)	0.121(12)
$A_4\pi(110)$	0.155(16)	0.755(19)	0.273(30)	0.713(20)	0.217(6)	0.94	0.139(8)	0.113(14)
$A_i\pi(100)$	0.244(23)	0.635(15)	0.219(15)	0.621(12)	0.097(3)	0.98	0.101(6)	0.093(8)
$A_i\pi(110)$	0.155(16)	0.755(19)	0.173(35)	0.743(34)	0.119(5)	0.98	0.108(9)	0.101(22)
			$\kappa_d = 0.157$; 32 $16^4 \to 16^3 \times 32$ lattices					
	6–14		8–15		7–14			
	1.68		1.23		1.44			
$A_4 A_4(000)$	0.049(3)	0.355(9)	0.096(6)	0.360(9)	0.192(2)	1.01	0.101(4)	0.103(8)
	7–14		6–13		4–10			
	1.38		2.66		3.82			
$A_4\pi(000)$	0.291(16)	0.360(7)	0.232(13)	0.361(7)	0.080(1)	1.00	0.102(3)	0.101(6)
	9–15		6–13		8–15			
	0.41		1.32		1.76			
$A_4\pi(100)$	0.127(8)	0.499(12)	0.175(14)	0.505(11)	0.144(4)	1.01	0.099(5)	0.099(9)
	7–16		6–13		7–13			
	1.46		0.87		1.48			
$A_4\pi(110)$	0.078(28)	0.658(54)	0.193(22)	0.664(17)	0.225(18)	1.01	0.110(22)	0.120(26)
	9–15		6–13		4–10			
	0.41		0.38		1.52			
$A_i\pi(100)$	0.127(8)	0.499(12)	0.132(11)	0.513(14)	0.094(3)	1.03	0.088(5)	0.097(9)
	7–16		6–13		8–15			
	1.46		0.83		0.78			
$A_i\pi(110)$	0.078(28)	0.658(54)	0.066(10)	0.590(24)	0.155(16)	0.90	0.113(24)	0.062(15)

tors to be correspondingly subject to noise. Deviations from Euclidean symmetry will also become more significant. In order to investigate these effects it is informative to examine the extent to which the usual continuum mass-shell condition $[E(\mathbf{p})^2 = m^2 + \mathbf{p}^2]$ holds, and whether the correlators satisfy the appropriate dispersion relation. In Fig. 3 we show a typical example of the dispersion relation for the pion, where the fitted value of $E(\mathbf{p})^2$ is plotted against $\mathbf{p}^2$. The solid line is the continuum dispersion relation, using the mass obtained at $\mathbf{p} = 0$. We find that, except for the coarsest lattices ($\beta = 5.4$ and $\kappa = 0.16$), the two lowest momenta are in good agreement with the continuum dispersion relation.

With this favorable result, we are now in a position to discuss the determination of $\langle \xi^2 \rangle$ by the method outlined earlier, which requires that we compute correlators at nonzero momentum. The results for $\langle \xi^2 \rangle$ from the four different ratios are contained in Table V. A measure of the quality of the data on the $16^3 \times 32$ lattice can be seen in Figs. 4 and 5, where we show R_4^{433} and R_4^{423} at $\kappa = 0.157$, $\beta = 5.6$ as a function of the time slice, together with the fit to the data. The data are of comparable quality at all values of the parameters used in the simulations, except at $\kappa = 0.156$, $\beta = 5.6$, where we were unable to find

TABLE V. The estimated value of $\langle \xi^2 \rangle$, using the ratios defined in Eq. (3.3) at the various parameters used in the simulation. There is no credible signal in $R_{4,3}^{433}$ at $\beta = 5.6$ and $\kappa = 0.156$.

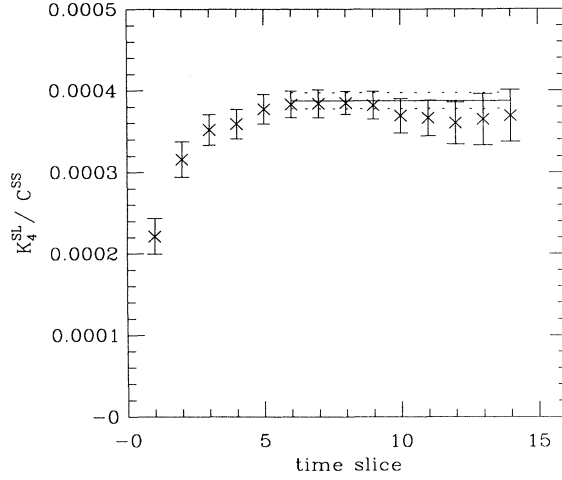|	$\langle \xi^2 \rangle$ from $n_j = 2$ Wilson fermions							
	$\beta = 5.4$ $\kappa = 0.160$	$\beta = 5.4$ $\kappa = 0.161$	$\beta = 5.4$ $\kappa = 0.162$	$\beta = 5.5$ $\kappa = 0.158$	$\beta = 5.5$ $\kappa = 0.159$	$\beta = 5.5$ $\kappa = 0.160$	$\beta = 5.6$ $\kappa = 0.156$	$\beta = 5.6$ $\kappa = 0.157$
$R_4^{433}/p_3 p_3$	0.077(5)	0.085(9)	0.092(4)	0.081(11)	0.116(10)	0.081(15)		0.097(10)
$R_4^{423}/p_2 p_3$	0.103(7)	0.133(6)	0.092(11)	0.071(21)	0.139(19)	0.130(18)	0.065(6)	0.099(16)
$R_3^{433}/p_4 p_3$	0.095(6)	0.099(12)	0.106(6)	0.103(19)	0.134(10)	0.095(15)		0.100(13)
$R_3^{423}/p_4 p_2$	0.119(12)	0.145(10)	0.104(10)	0.085(26)	0.152(9)	0.127(23)	0.095(10)	0.102(17)

FIG. 1. The ratio of K_4^{SL} and C^{SS} are shown at $\beta=5.5$ and $\kappa=0.160$ on the $16^3\times32$ lattice. The pion operator used is the pseudoscalar density. The solid line spans the range of the fit and is the quoted value, and the dashed lines represent the errors on the fit.
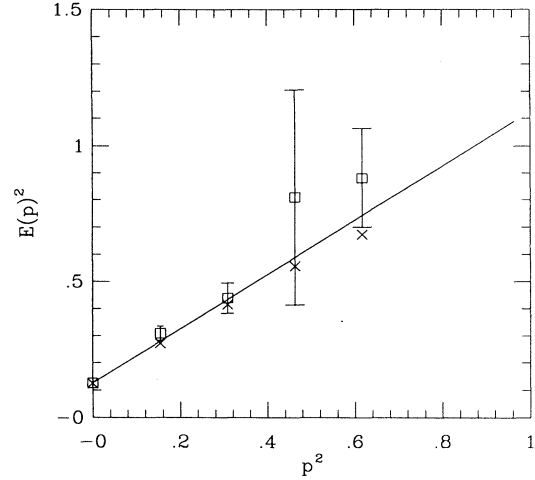

FIG. 3. The measured value of $E(\mathbf{p})^2$ is shown versus $\mathbf{p}^2$ at $\beta=5.5$ and $\kappa=0.160$ on a $16^3\times32$ lattice, determined by a single-particle fit to the correlator $C^{SS}(t,\mathbf{p})$. The solid line is the continuum dispersion relation $E(\mathbf{p})^2=m^2+\mathbf{p}^2$, where m is the energy at $\mathbf{p}=0$. The crosses give the lattice dispersion relation for a free boson.

a signal in K_{433}. In Table VI we also give the raw data for the ratios R at the lightest value of pion mass at each value of β, along with the fit range used and the χ^2/N_{DF} achieved. For the ratios R_4^{433} and R_4^{423} the quoted χ^2 also applies to the estimate of $\langle\xi^2\rangle$, since this is obtained by dividing by the constant $\pi^2/64$.

Once again, the cumulative data are best expressed as a function of $(m_\pi/m_\rho)^2$, which we show in Figs. 6 and 7 for $R_{4,3}^{433}$ and $R_{4,3}^{423}$, respectively. The results are more consistent for $R_{4,3}^{433}$. In contrast with quenched simulations, where measurements are made at various values of

κ but on the same set of lattices, these data points are completely uncorrelated. It is not known *a priori* how the data should behave as a function of the quark mass, and from our data it is difficult to draw any conclusions. However, if we assume that $\langle\xi^2\rangle$ is constant with m_π/m_ρ, then we obtain

$$\langle\xi^2\rangle_{latt}=0.10(1)\quad\text{using }R_{4,3}^{433},$$
$$\langle\xi^2\rangle_{latt}=0.11(2)\quad\text{using }R_{4,3}^{423}.$$

$$(4.1)$$
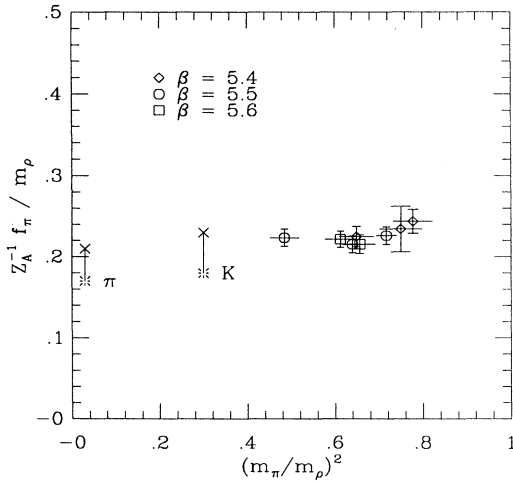
It should be noted that the renormalization constants for

FIG. 2. The ratio $Z_A^{-1}f_\pi/m_\rho$ is shown against the ratio $(m_\pi/m_\rho)^2$. Also shown is the physical value of the ratios for the pion and kaon and their value rescaled by $Z_A=0.8$.
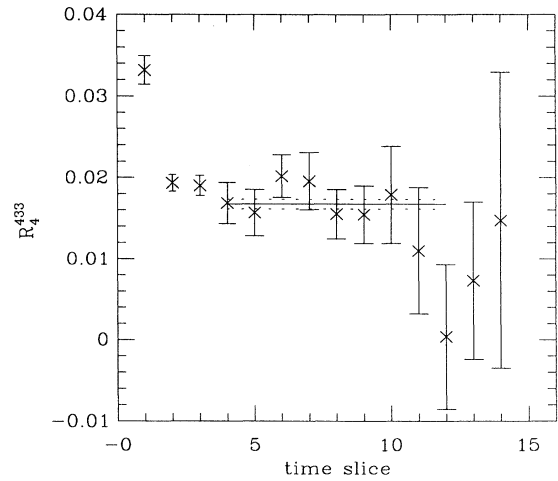

FIG. 4. R_4^{433} is shown at $\beta=5.6$ and $\kappa=0.157$ on the $16^3\times32$ lattice. The solid line spans the range of the fit and is the quoted value, and the dashed lines represent the errors on the fit.
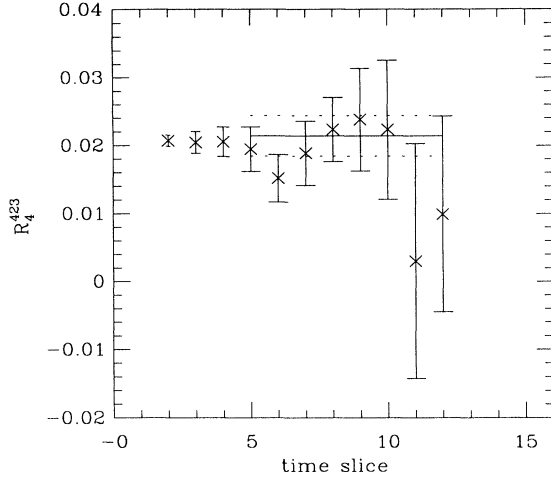
FIG. 5. R_4^{423} is shown at $\beta=5.6$ and $\kappa=0.157$ on the $16^3 \times 32$ lattice. The solid line spans the range of the fit and is the quoted value, and the dashed lines represent the errors on the fit.
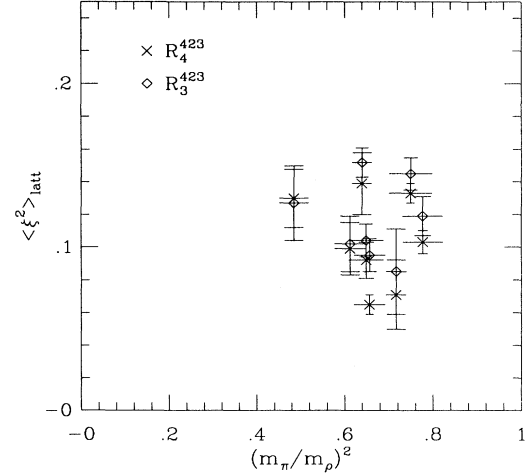

FIG. 7. The measured value of $\langle \xi^2 \rangle$ determined using R_4^{423} (crosses) and R_3^{423} (diamonds) is shown against $(m_\pi/m_\rho)^2$.

these two operators may differ.

What is clear from the mean quoted in Eq. (4.1) and from the spread in the data is that our estimates are considerably smaller than those of previous studies [see Eq. (1.5)]. We believe that the major cause of the improvement is the use of smeared propagators and a larger lattice volume.

V. CONCLUSIONS

Using a variety of lattice parameters, and including the effects of two flavors of Wilson fermions, we have measured f_π and the second moment of the quark distribu-

tion amplitude in the pion, $\langle \xi^2 \rangle$. Both of these measurements require that we extract the residue of the pion's contribution to various correlators. The use of smeared sources has allowed this to be done more cleanly than before.

For f_π we see approximate momentum independence for the three momenta considered. The actual value of f_π for all three values of β agrees well with the physical value assuming a lattice renormalization constant for the axial-vector current of around 0.8.

Our measurements of $\langle \xi^2 \rangle$ suggest that the fractional light-cone momenta of the pion is more evenly divided between the component quark and antiquark than previous studies, using both sum rules and quenched lattice QCD, have indicated.
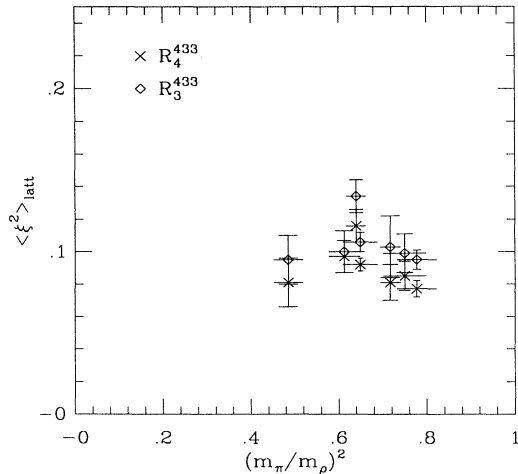

FIG. 6. The measured value of $\langle \xi^2 \rangle$ determined using R_4^{433} (crosses) and R_3^{433} (diamonds) is shown against $(m_\pi/m_\rho)^2$.

TABLE VI. The measured values of the ratios R defined in Eq. (3.3) for the largest value of κ at each value of β. Above each number we also quote the fit range used and the χ^2 per degree of freedom achieved in the fit.

Ratio	$\beta=5.4$ $\kappa=0.162$	$\beta=5.5$ $\kappa=0.160$	$\beta=5.6$ $\kappa=0.157$
	5–12	7–14	6–12
	1.45	1.11	1.79
$R_4^{433} \times 10$	0.141(6)	0.125(23)	0.149(16)
	5–10	5–11	6–12
	1.82	1.95	2.95
$R_4^{423} \times 10$	0.142(17)	0.201(28)	0.151(25)
	5–10	8–12	6–13
	0.96	1.10	1.25
$R_3^{433} \times 10$	0.279(14)	0.182(30)	0.201(3)
	5–10	5–11	6–12
	1.80	2.05	3.77
$R_3^{423} \times 10$	0.316(30)	0.304(55)	0.236(39)

*Current address.

[1] G. P. Lepage and S. J. Brodsky, Phys. Rev. D **22**, 2157 (1980); A. V. Radyushkin, Dubna Report No. OIYaI R2-10717, 1977 (unpublished).

[2] V. L. Chernyak and A. R. Zhitnitsky, Phys. Rep. **112**, 174 (1984); Nucl. Phys. **B201**, 492 (1982).

[3] S. V. Mikhailov and A. V. Radyushkin, Yad. Fiz. **49**, 794 (1989) [Sov. J. Nucl. Phys. **49**, 494 (1989)].

[4] N. Isgur and C. H. Llewellyn-Smith, Phys. Rev. Lett. **52**, 1080 (1984); Nucl. Phys. **B317**, 526 (1989).

[5] G. Martinelli and C. T. Sachrajda, Phys. Lett. B **190**, 151 (1987); Nucl. Phys. **B306**, 865 (1988).

[6] T. A. DeGrand and R. D. Loft, Phys. Rev. D **38**, 954 (1988).

[7] A. S. Kronfeld and D. Photiadis, Phys. Rev. D **31**, 2939 (1985); S. Gottlieb and A. S. Kronfeld, *ibid.* **33**, 227 (1985).

[8] L. Maiani and G. Martinelli, Phys. Lett. B **178**, 265 (1986).

[9] S. Duane, A. D. Kennedy, B. J. Pendleton, and D. Roweth, Phys. Lett. B **195**, 216 (1987).

[10] C. Baillie, R. Brickner, R. Gupta, G. Kilcup, A. Patel, and S. Sharpe, Los Alamos Report No. LA-UR-91-528 (unpublished).

[11] S. Güsken, in *Lattice '89*, Proceedings of the International Symposium, Capri, Italy, 1989, edited by R. Petronzio *et al.* [Nucl. Phys. B (Proc. Suppl.) **17**, 361 (1990)].

[12] S. Gottlieb, P. B. Mackenzie, H. B. Thacker, and D. Weingarten, Nucl. Phys. **B263**, 704 (1986).